Proceedings of the Indian National Science Academy (2023) 89:891–901
https://doi.org/10.1007/s43538-023-00205-6

RESEARCH PAPER

Assessment of abdominal rehabilitation for diastasis recti abdominis using ensemble autoencoder

Menaka Radhakrishnan[1] · Vinitha Joshy Premkumar[1] · Mohan Teja Guddimettla[2] · Sanjucta Choudhury[2] · Siddharth Basu[2] · Satvik Gupta[2]

Received: 20 January 2023 / Accepted: 26 August 2023 / Published online: 12 September 2023

Abstract

Women experience major bodily changes both during pregnancy and post-pregnancy. Diastasis Recti Abdominis (DRA) is a noticeable issue in the postpartum period among the female population in the world. Though postnatal fitness has gained attention in the recent decade, there is scarce knowledge of the abnormal condition called DRA and its consequences. In the presence of an abnormality, women feel less energetic in their daily activities and may experience fatigue in the abdominal muscles. The physical way of regaining strength in core abdominal muscles includes rehabilitation through exercises prescribed by physiotherapists. The sit-up and curl-up exercises engage the core abdominal muscles and when practiced regularly can bring back the separated recti muscles together in time. In order to bring this practice unsupervised by the physicians and monitor the pace of exercises by the patient individually, wearable Inertial measurement unit (IMU) sensors were employed. The utilization of IMU wearable sensors for DRA has been sparsely explored in literature. In this study, two groups of subjects with DRA perform the rehabilitation exercises and respective inertial measurements were observed. When the situation goes unsupervised, the effective contraction of the abdominal recti muscles and the correctness of exercises were uncertain. It's a well-known fact that deep learning algorithms aid in determining the significant features thereby making the unsupervised classification problem more efficient. Here in this study an ensembled autoencoder neural network is implemented in which the IMU datasets were employed for the classification of correct and incorrect exercises. The latent vector generated in the autoencoder model encapsulates the inherent patterns of the input by undertaking all occurrences into a latent space. Thereby in this work, the reconstruction error generated from the autoencoder network is used to determine the correct and incorrect exercise. The ensemble approach, grouping two classes of autoencoders provides a model with higher predictivity.

Keywords Diastasis recti abdominis · Inertial measurement sensors · Ensemble · Autoencoder · Latent vector

Introduction

The term "Diastasis Recti Abdominis" refers to a disorder in which both rectus abdominis muscles separate and move to the sides, along with an expansion of the linea alba tissue and a bulging of the abdominal wall. DRA is prevalent among women during pregnancy and the postpartum period (Engh et al. 2020). The divarication of the rectus abdominis muscle brought on by the stretching and expansion of the linea alba subsequently increases the inter-recti distance (IRD). DRA is developed as a result of mechanical and functional issues with the anterior abdominal wall. It happens when the recti muscles separate excessively and fail to reattach even eight weeks after delivery. Three months after giving birth, 33% of women have DRA (Radhakrishnan and Ramamurthy 2022; Menaka et al. 2023). Postpartum women were most frequently affected by DRA. For those who experience it, it is extremely uncomfortable. Many women claim that after becoming pregnant, their bodies no longer feel the same way, and because of an unsteady feeling in the middle of their belly, they sometimes have trouble moving around. Although most women experience the condition in third trimester of pregnancy, over 40% women still have the condition even after many

✉ Menaka Radhakrishnan
menaka.r@vit.ac.in

1 Centre for Cyber Physical Systems (CCPS), School of Electronics Engineering, Vellore Institute of Technology, Chennai 600127, India

2 School of Electronics Engineering, Vellore Institute of Technology, Chennai 600127, India

years of pregnancy and childbirth. Despite the condition's great incidence, not much research has been done in this field. The structures of the abdominal wall have undergone a biomechanical alteration as a result of the increased inter-recti distance. Findings imply that abdominal muscular function is adversely affected by the presence of an elevated IRD in postpartum (Eriksson Crommert et al. 2020). According to certain views, failing to treat DRA effectively might result in long-term consequences such as aberrant posture (Boissonnault and Blaschak 1988), lumbopelvic pain, and cosmetic flaws (Britnell et al. 2005). To our knowledge, these claims were not supported by any high-caliber clinical research (Da Mota et al. 2015).

Hence DRA has to be identified as early as possible in order to prevent further dysfunctions. Figure 1 shows the view of abdomen without DRA and with DRA. Estimates show that four out of ten women still experience low back and pelvic pain six months after giving birth. Diastasis recti abdominis, which affects many postpartum women, seldom goes away on its own and may last for years. Postnatal women with DRA seek medical attention when the abnormality worsens and in some cased DRA is identified during postnatal check-ups and examinations. Hence as the first step of treatment physiotherapists suggest rehabilitation exercises engaging the core abdominal muscles. The deep core stabilizing muscles, also known as the transversus abdominis, pelvic floor, deep multifidus, and diaphragm form a muscular cylinder that supports the spine and the pelvis. The sit-up and curl-up exercises were the common exercises that efficiently work on the transverse abdominis and pelvic floor muscles. Women were advised to practice abdominal workouts regularly to reduce the IRD in meantime. Other non-surgical therapies that were frequently utilized for women with DRA include aerobic workouts, education about proper posture and back care, and external support (such as a corset or Tubigrip).

Modern marker-based optical motion capture systems were extremely precise, but due to the high cost and specialized knowledge needed for operation and maintenance, they were not ideal for telerehabilitation. Additionally, due to the compact spaces and furniture in homes, the operational environment is restricted to a certain room, and the markers were readily obscured. IMU-based solutions get around issues with occlusion and illumination that were common with optical motion capture systems (Qaroush et al. 2021). This IMU-based human motion capture system's accuracy has been demonstrated in earlier studies to be sufficient for event detection and feature extraction in walking rehabilitation (Chiarello et al. 2005). IMU sensors were deployed in robotic arm with data processing and acquisition in the form of EMG (Electromyography) and IMU and online data monitoring data had been developed (Lopes et al. 2017). The robotic arm is capable of operating in both a virtual and real environment (Thabet and Alshehri 2019; Kong et al. 2013). Wearable rehabilitation devices can be made from inertial movement units (IMUs) which were wireless transmission devices that were lightweight, affordable, and energy-efficient (Patelet al. 2012; Ahmad et al. 2013). As a result, IMUs can take the place of kinect in the detection of human activities (Ganesan et al.2015; Du et al. 2018). Over the last decade, technological advancements have resulted in enormous strides in MEMS (Micro-Electro-Mechanical Systems) IMU manufacturing. As a result, the size and cost of IMUs were decreasing, while their accuracy and performance were improving. This is one of the primary reasons for the widespread use of low-cost IMUs (Al-Azzawi et al.2021; Pintelas and Livieris 2020; Štebe et al. 2021).

In machine learning, classification is one of the most well-known and extensively researched tasks (Al-Azzawi et al.2021; Al-Ezzi et al. 2022; Chowdhury et al. 2021; Boukhennoufa et al. 2022; Radhakrishnan et al. 2022). To anticipate the characteristics of new patterns, a classifier

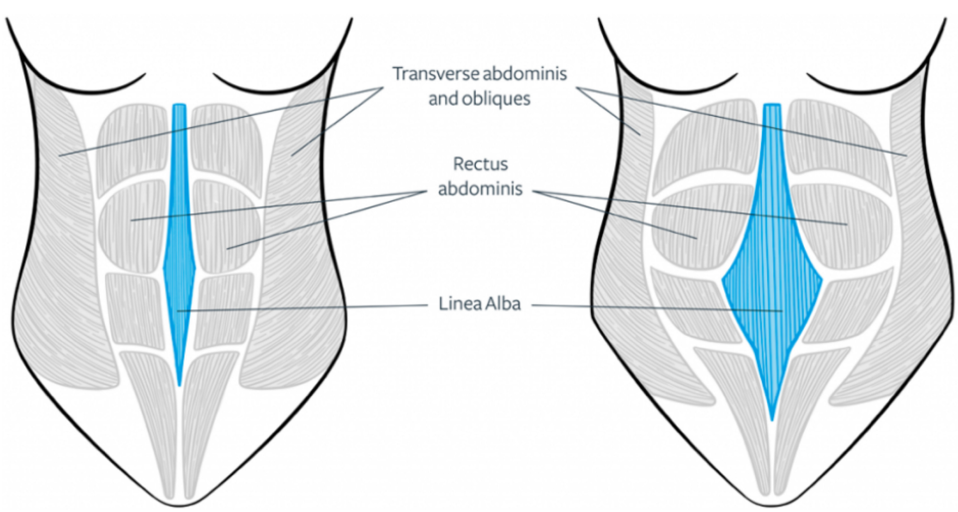

Fig. 1 Abdomen—without and with Diastasis Recti

analyzes a set of training cases to extract pertinent data. Different methods may be used to classify data. Particular classifiers include the Multi-Layer Perceptron (MLP), k-Nearest Neighbors (kNN), Support Vector Machines (SVM), and C4.5 decision tree (Pulgar et al. 2021). Deep neural network (DNN)-based feature representation learning has grown in prominence in the area of machine learning (ML) in recent years. A DNN has numerous hidden layers and can learn high-level abstract data features using a layer-by-layer nonlinear transformation based on extensive training data. Deep learning technology is better equipped to describe the rich intrinsic information included in data due to the usage of a complex hierarchical structure and layer-by-layer feature modification (Li et al. 2021). Deep learning techniques have lately been employed for their detection using statistics and machine learning. Outlier or anomaly detection is used in many different fields, hence there has been a lot of research in this area.

Supervised learning is the most robust tool of Artificial Intelligence (AI) and has served in code recognition, speech recognition, image processing and understanding of human genetics. However, this approach less relies upon recent problems. Unsupervised learning, being expertise in the automatic representation of features is highly useful in solving the difficult problems of AI. Recently, autoencoders and other generative models have received a lot of attention in unsupervised learning issues (Han et al. 2020; Liu et al. 2021). From these studies, compact representations can be built to describe the generative process for unlabelled data (Chaurasia et al. 2020). A multilayer network with a sparse autoencoder at each layer is known as a stacked autoencoder (Kadam and Jadhav 2019; An et al. 2022; Pulgar et al. 2021; Saha et al. 2021). Compared to a shallow single-layer autoencoder, it aids in the identification of more sophisticated and effective predictors from different variables.

Materials and methods

The DRA datasets were acquired from 20 parous female patients during the hospital organised medical camp. The research study's inclusion criteria were narrowed down to women with moderate to severe discomfort between six months after delivery and three years after delivery. All 20 female subjects were assessed by the physical therapists. DRA examination was performed for all the subjects. The informed consents were obtained from all the subjects and the data collection protocol was approved by Institutional Ethics Committee. The data was acquired for the subjects separated in two groups. Subjects in group 1 were well trained with rehabilitation exercises and subjects in group 2 were new patients performed the exercises without training. The datasets were thereby obtained for correct and incorrect exercises.

Data acquisition

During the camp, the subjects were initially obtained with the basic parameters like age, BMI (Body Mass Index obtained from height and weight), number of pregnancies, duration after delivery. They were then asked to perform the Partial curl up test. The Partial curl up test is the fitness test which was carried out to estimate the DRA and associated conditions. Table 1 is given with data acquisition details of the recruited subjects. DRA is confirmed with the measurement of inter-recti distance (IRD) using vernier callipers. Rehabilitation exercises were suggested by the medical professionals for the subjects and asked to perform to mention the importance of its correctness as incorrect exercises lead to ineffective contractions. The curl-up and sit-up exercises strengthen the abdominal core muscles. For each patient, the IMU datasets were collected for curl-up and sit-up exercises. The flow of each exercise was executed as sit-up/curl-up position, holding the position for 10 counts and relaxing to normal. Three repetitions of each exercise flow have been followed to acquire a single dataset. Approximately it takes 40–60 s to acquire a single dataset.

To estimate the correctness of the performance of exercises, the IMU sensors were placed in the abdominal region of the patient and the respective readings were obtained as shown in Fig. 2. Shimmer IMU sensor device was used to acquire the IMU signals for this work.

Rehabilitation exercises were suggested for the patients to maintain abdominal fitness after delivery and also predominantly to reduce the inter-recti distance. In this work, two rehabilitation exercises namely sit-up and curl-up as shown in Fig. 3 were considered for the study. Sit-ups were abdominal exercises that were practiced for gaining abdominal strength. The patient was allowed to lie flat with both legs bent in an inclined position to reduce stress in the backbone. The exercise begins with a slight lift in the head. This position was on hold for 10 counts and relaxed back to flat back position. During the exercise the contraction of abdominal recti muscles happens and then it was done continuously along with the breathing pattern which has been proved to improve the inter recti distance in postnatal women. Curl-ups were exercises commonly practised for the endurance of abdominal muscles and core stability. The exercise begins with legs bent and a curl up of the head with chins towards the chest until the upper back was off the floor. The position is on hold for 10 counts and relaxed back to flat back position. It was carried out along with the breathing pattern and this exercise has also been proven for core stability and reducing IRD for diastasis recti abdominis. The analysis of

Table 1 The data acquisition details of the recruited subjects

Groups	S. no	Patients	Age	BMI	No. of pregnancies	Duration after delivery	Partial Curl up test Average—(25–30)
Group 1	1	Patient 1	23	31.5	1	45 days	14
	2	Patient 2	27	25	1	7 months	14
	3	Patient 3	29	30	2	2 years 3 months	24
	4	Patient 4	26	28	1	19 months	25
	5	Patient 5	28	29	1	11 months	20
	6	Patient 6	32	32	2	2 years	15
	7	Patient 7	27	25.5	1	6 months	14
	8	Patient 8	28	24	1	60 days	26
	9	Patient 9	28	26	2	45 days	18
	10	Patient 10	25	29	1	3 months	25
Group 2	11	Patient 11	26	29.5	1	45 days	28
	12	Patient 12	31	28	2	45 days	20
	13	Patient 13	29	26	1	4 months	15
	14	Patient 14	26	30.5	1	1 year	29
	15	Patient 15	27	28	1	48 days	18
	16	Patient 16	29	26	1	1 year 6 months	27
	17	Patient 17	31	24	2	1 year 2 months	24
	18	Patient 18	26	28.5	1	6 months	25
	19	Patient 19	29	30.5	1	3 months	24
	20	Patient 20	35	30	3	2 years	20

Fig. 2 IMU sensor in data acquisition

the exercises for various patients has been performed for the effective evaluation of correct and incorrect exercises.

IMU sensors were composed of Micro electro-mechanical system-based sensors including accelerometer, gyroscope and a magnetometer. The sensors perform the measurements in 3 directions described as X, Y, and Z positions. When the exercises were performed, inertial acceleration occurs, as the abdominal muscles move in accordance to the force during the voluntary action. This acceleration is the measure of rate of change of velocity given in units of m/s. The gyroscope measures the angular velocity which is the rate at which the

Fig. 3 Sit-up and Curl-up exercises

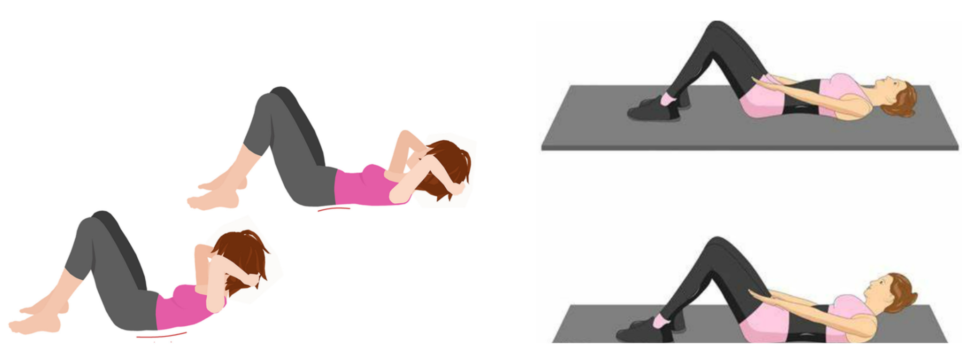

abdominal muscles move in terms of speed and axis of rotation measured in units of deg/sec. The magnetometer measures the magnetic flux which is the direction and strength of local magnetic field. The technical specification of an IMU sensor is given in Table 2. Figure 4. shows the IMU data acquisition while the patient is performing exercises.

The erratic character of IMU signals has been reduced by the calibration of sensors. The sampling frequency for IMU data acquisition is set at 51.2 Hz as the values of IMU components clearly fall within the range. The IMU signals' spectrum analysis suggests that for optimal performance, a sampling rate of 20–50 Hz was optimum for detecting human activity (Antonio Santoyo-Ramón et al. 2022). Table 2 describes the hardware specifications of the accelerometer, gyroscope and magnetometer in the Shimmer3 IMU sensor unit. Using the Python platform, TensorFlow, NumPy and the pandas module, the IMU signals were processed. For data processing and categorization issues based on machine learning, these libraries were crucial resources (Fig. 5).

Table 2 The technical specifications of an IMU sensor

Feature	Specification
Accelerometer	
Source	ICM-20948 Accelerometer
Range	± 2 g
Channels	Triaxial (x, y, z)
Sampling rate	51.2 Hz
Numeric resolution	16 bits, signed
Typical operating current	68.9 µA
Gyroscope	
Source	ICM-20948 Gyroscope
Range	± 250; ± 500; ± 1000; ± 2000 dps
Channels	Triaxial (x, y, z)
Sampling rate	51.2 Hz
Numeric resolution	16 bits, signed
Typical operating current	1.23 mA
Magnetometer	
Source	ICM-20948 Magnetometer
Range	± 4900 µT
Channels	Triaxial (x, y, z)
Sampling rate	51.2 Hz
Numeric resolution	16 bits, signed
Typical operating current	1.23 mA

Unsupervised classification for assessment of rehabilitation exercises

An autoencoder functions as an unsupervised neural network, comprising an encoder and a decoder as shown in Fig. 6. The input to the autoencoder was converted into a latent vector with a desirable dimension. The significant features were learned automatically by the encoder network and stored as a latent vector. Later this vector was reconstructed to produce an output that was of the same size as the input. The encoding part of the network has comparatively a smaller number of hidden units in each layer and as a result, this section was constrained to select only the most important and representative data aspects. The decoding part of the network was carried out as the next part of the network which works to decode the encoded data using a higher number of hidden units in each layer to reconstruct the original input.

The data collected from IMU wearable sensors were fed as input to the autoencoder neural network. The autoencoder learns the compact representation of the given IMU signals which converts the high-dimensional continuous data to low-dimensional data by the process of encoding. The latent space was generated which signifies the features derived from the input signal after the stage of encoding. Decoding the features from the latent vector generates the reconstruction of an input signal. The autoencoder model learns the data feature and simplifies the representation for easier analysis. The reconstruction errors signify the detection of correct and incorrect exercises. The ensemble of Autoencoders was used for Sit-up and Curl-up exercises. Figure 5 shows the basic block diagram of the proposed work.

An autoencoder is defined by two sets: the space of encoded messages X and the space of decoded messages Z where both X and Z belong to Euclidean spaces $X \in R^m$ and $Z \in R^n$ for some m, n and two parameterized functions or families. The encoder network E_Φ: $X \to Z$ and D_Φ: $Z \to X'$. For any $x \in X$ we write $z = E_\Phi(x)$ where z is called the encoded message or the latent space variable, latent

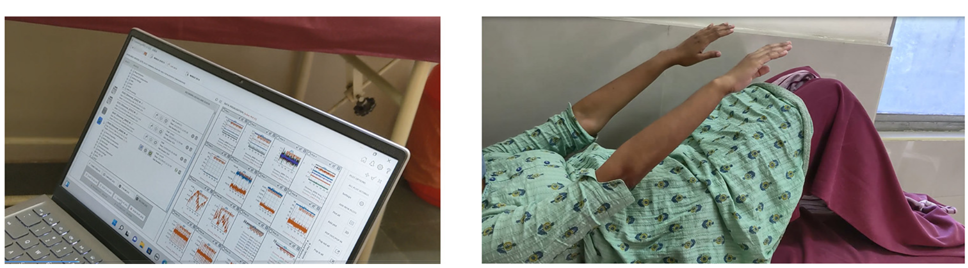

Fig. 4 Data acquisition and patient performing the rehabilitation exercise

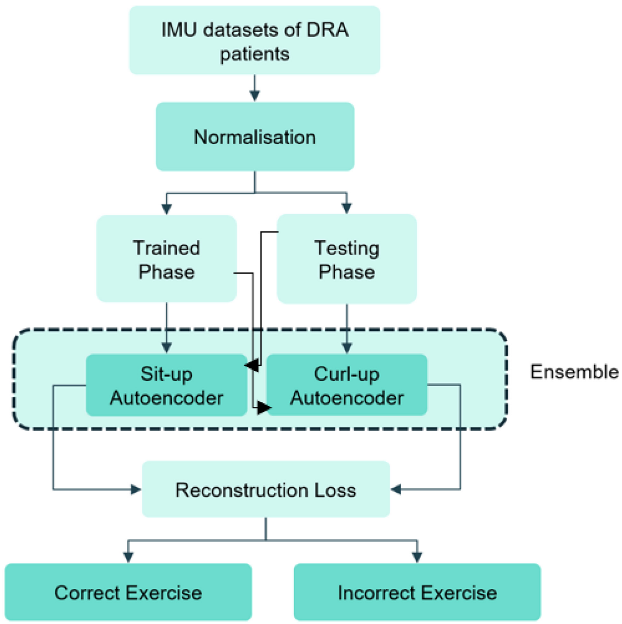

Fig. 5 Basic block diagram of the proposed work

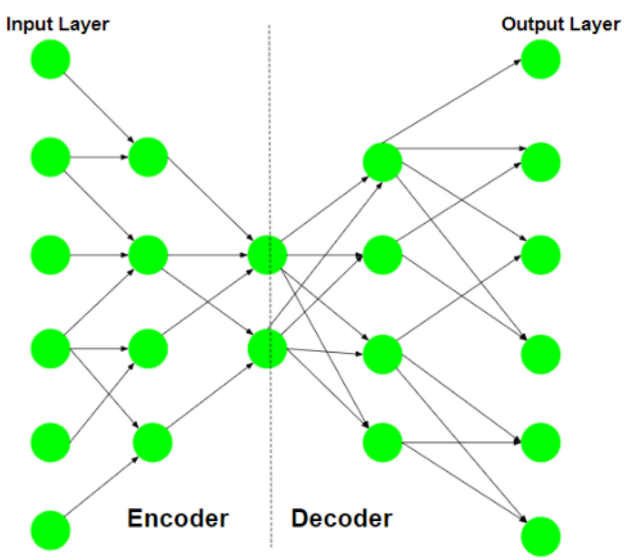

Fig. 6 Representation of autoencoder

representation, latent vector etc. Conversely, for any $z \in Z$ we write $x' = D_{\Phi}(z)$ Where x' is called the decoded message.

Parameterization

The code size, number of layers, number of nodes, and loss function were the hyperparameters as shown in Fig. 7 whose values control the learning process and need to be set before the training phase. The code size or the size of the latent vector is smaller than the input vector size and results in good

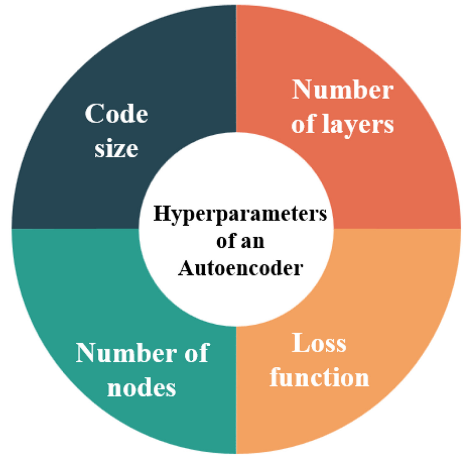

Fig. 7 Hyperparameters of an autoencoder

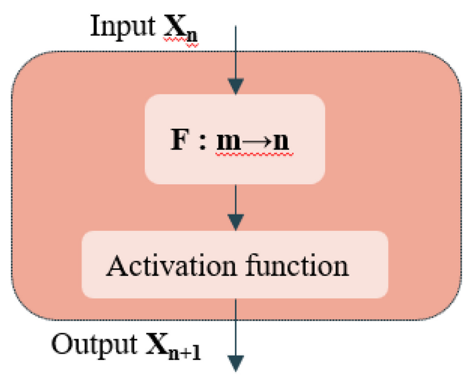

Fig. 8 Representation of Activation function

compression. The network's performance is also governed by the number of layers deployed. With each additional layer of the encoder, the number of nodes per layer decreases and then increases in the decoder. In terms of the layer structure, the decoder is symmetric to the encoder. Mean squared error (MSE), a loss function used in machine learning, is used to assess predictive models. The average squared error between the anticipated value and the actual value is what MSE calculates.

Each encoder and decoder network is further divided into dense layers with different activation function shown in Fig. 8 such as ReLU and sigmoidal activation functions each dense layer is of form

$$L_{\Phi} : X_n \rightarrow X_{n+1} \quad (1)$$

where $X_n \in R^m$ and $X_{n+1} \in R^n$ for some m, n in encoder part for every layer $m > n$ with activation function at the end of it we majorly used 2 activation functions namely relu activation layer and sigmoidal activation layer.

Sigmoidal activation function A sigmoid function is a mathematical function having a characteristic "S"-shaped curve or sigmoid curve. A common example of a sigmoid function is the logistic function a logistic function is given by

$$S(x) = ex/(e^{x} + 1) \tag{2}$$

ReLU activation function In the context of artificial neural networks, the rectifier or ReLU (Rectified Linear Unit) activation function is an activation function defined as the positive part of its argument:

$$F(x) = x^{+} = \max(b * x,\ a * x) \text{ usually } b = 0 \text{ and } a = 1 \tag{3}$$

For the given use case ReLU activation function showed the best results.

The more complex the network architecture and learning manner, the higher possibility that the network overfits with data and the more challenging the assessment of feature contribution, respectively. In this work, we consider simple AEs with input and output layers together with a varied unit number in the hidden layer. In this way, we can evaluate the stability of the features with small changes in the network architecture before approaching more complex architectures. For the activation function, we select a logistic sigmoid function that likely relates to a non-linear relationship in exercises. The connection weights learned from AEs were then used as initial weights for the classifier network.

The two interesting practical applications of autoencoders were data denoising and dimensionality reduction for data visualization**.** With appropriate dimensionality and sparsity constraints, autoencoders can learn data projections that were more interesting than PCA or other basic techniques. In an Autoencoder network, the network is trained with inputs and the model precisely learns the most frequently observed characteristics of salient features. Hence for the wrong exercises, the reconstruction performance was degraded. The correct exercise data only was used to train the autoencoder because if both correct and incorrect data were used to train the autoencoder network, the frequency of detection of incorrect exercise was less. After training, the AE accurately reconstructs the correct exercise but fails to do it along with the incorrect exercise. Reconstruction error was the error between the original data and the reconstructed data (from latent vector) was used as a score to classify the correct and incorrect exercises.

Ensembled approach

In this work, a set of autoencoders were deployed as an ensemble for classification. The major benefit of using an ensembled algorithm was the ability to overcome noise, bias and variance, hence there was an improvement in prediction performance. In the training phase, the inputs were used to train one autoencoder per class. Thus, two classes of inputs were considered one for the sit-up exercise and the other for the curl-up exercise. Each autoencoder learns a different exercise in the training phase. In the testing phase, each Autoencoder tries to reconstruct the given input. When the autoencoder was given the wrong class as input the original input pattern was still reconstructed, but creates a lot of errors between the input and output. This fact was utilised to train autoencoders using an ensemble of these autoencoders and comparing the error with their training error. Classification was performed accordingly and the two error peaks were obtained. When all errors were consolidated, the first error peak was of the original subclass and second higher error peak was the other subclasses we make a threshold as we see fit between these error peaks and hence, we can differentiate between subclasses as well. The architecture was implemented for 2 exercises curl-up and sit-up which have further classes correct and not correct 2 autoencoders were assembled for each exercise with correct data and it's further used for evaluation (Figs. 9 and 10).

Results

Shimmer IMU was used to obtain the sensor data. For the sit-up and curl-up exercises that have been recorded as 9-column data of accelerometer, gyroscope, and magnetometer along directions X, Y, and Z, the sample size of the IMU dataset was between 1000 and 1500 data points. When the curl-up exercise data was given as training input to an autoencoder the network learns the input pattern with the encoder and reconstructs the inherited pattern

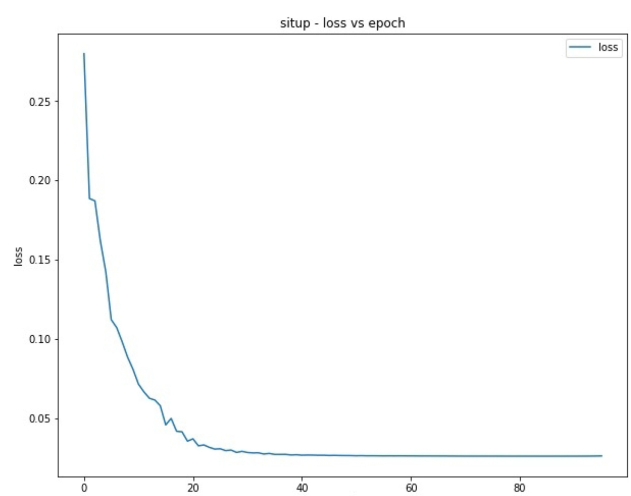

Fig. 9 Training loss

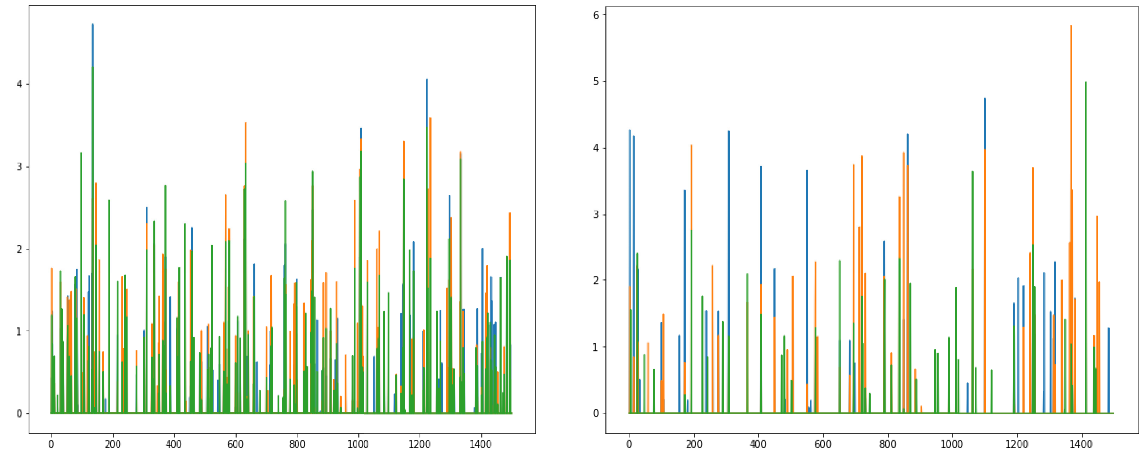

(a) (b)

X-axis- distribution of latent vector, Y-axis- latent space vector of length 1500

Fig. 10 Latent vector for **a** curl-up and **b** sit-up

to an output with the decoder which was of the same size as the input. The latent space can be set in the designed autoencoder model and here it was set as 1500. The graphs Figs. 11 and 12 shows the error between the input and output we can see that correct data has a significantly lower error and incorrect data has a significantly higher error using which we can differentiate if the exercise has been done correctly. For sit-ups also, the sit-up autoencoder performs well like the curl-up autoencoder we were also able to distinguish if the sit-up was performed correctly. If all of the data was passed through the curl-up autoencoder we can see only that it can differentiate between correct curl-up and remaining else. The plot of training loss is given in Fig. 9. The latent space vector for both curl-up and sit-up have very significant differences which can be seen in the graphs in Fig. 10.

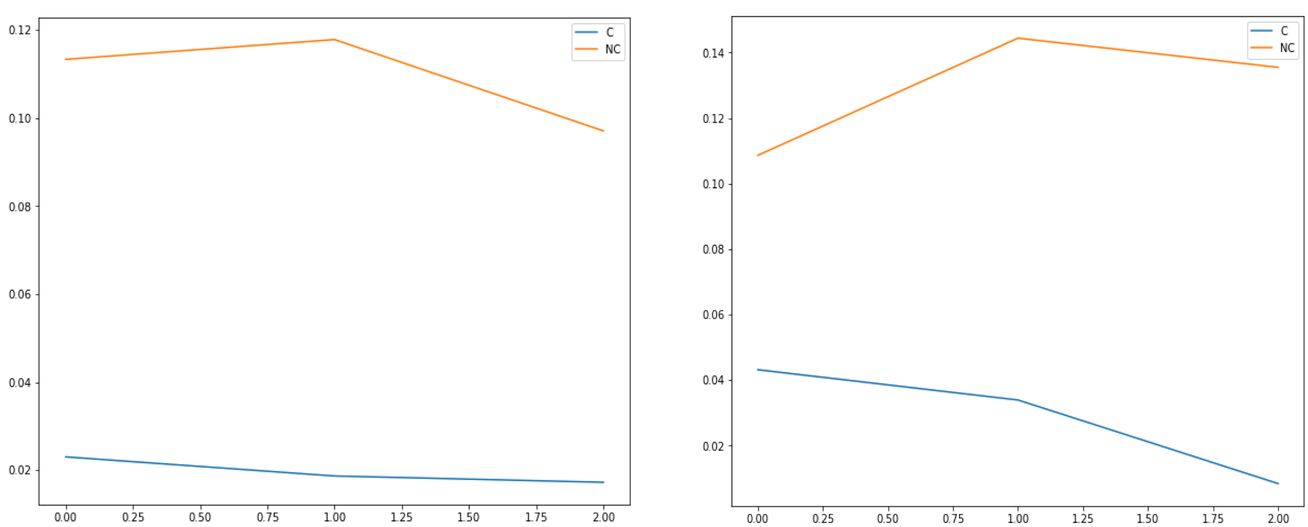

(a) (b)

Fig. 11 Plot of correct and incorrect exercises for **a** curl-up and **b** sit-up exercises. (y-axis represents the error range and x-axis represents the samples)

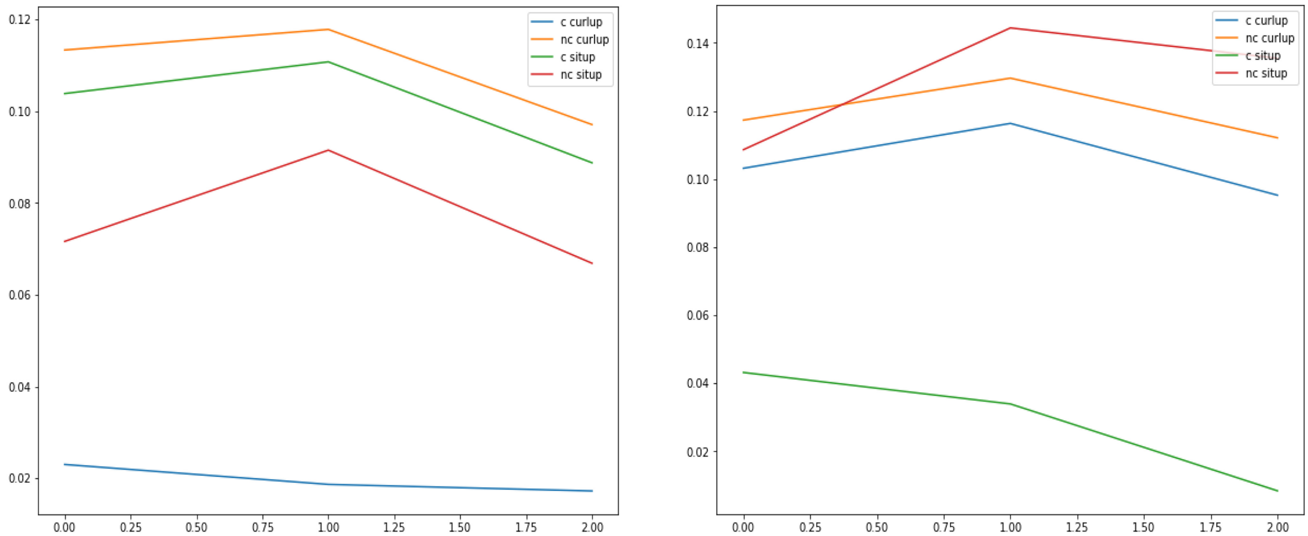

(a) (b)

Fig. 12 Plot of correct and incorrect exercises for training one exercise and testing both exercises. **a** Curl-up autoencoder **b** Sit-up autoencoder (y-axis represents the error range and x-axis represents the samples)

Discussions

Basically, autoencoders were utilized in the dimensionality reduction and other unsupervised problems. Since autoencoders perform better in higher n-dimensional settings, they could be a potential solution to the non-definitive principal components problem. A labelled dataset was not necessary for an AE to train. Additionally, Deep Neural Networks were the foundation upon which Autoencoders were formed. With substantially fewer reconstruction errors and information loss, this would improve the information extraction process even more. However, there were some drawbacks to using autoencoders such as overfitting if not trained with enough data, difficulty in training due to instability during the back-propagation step because only one direction information flow exists within each layer and also the computational cost due to time needed to encode/decode a larger volume of inputs. Despite all of these disadvantages, overall outcomes from employing autoencoders appear good so far as we keep learning more about their potential. In this work, autoencoder network was trained with the correct class of input and when the wrong class of input was given, the network will still try to make the original input pattern but creates lot of errors between the input and output. This fact was utilized for the application of classification of correct and incorrect exercises by training the autoencoders. This results in two error peaks and when all errors were consolidated the first error peak was of the original class and second higher error peak was the other class. By setting a suitable threshold between these error peaks, the correct and incorrect data were distinguished. The dataset was comparatively small to train and test the data using the model and with such less data the model can be overfitted. The ensembled model provides much more insight if adequate data has been used in future for the analysis.

Conclusion

The major goal of this research was to evaluate the effectiveness of abdominal rehabilitation exercises. Identifying the correctness of exercises aids the physiotherapists to regulate the patients through exercises to reduce the gap between the recti muscles thereby reducing IRD. The wearable IMU sensors were smaller, low cost, reliable and provides movements in 3D space with more Degree of Freedom (DOF). The acceleration, angular velocity and magnetic field information were acquired from the IMU sensor which tracks the movement information of the recti muscles. During rehabilitation exercises, there was a variation in the sensor readings according to the displacement of sensors in X, Y and Z directions. In this work, an autoencoder was designed for two exercises namely sit-ups and curl-ups. The Autoencoder Neural network employs the unsupervised way of classification of the correct and incorrect exercises. In each class of autoencoder, the input pattern was stored in latent space and thereby using the reconstruction error produced in each model determines the correct and incorrect exercises. The ensembled model utilises the combination of curl-up and sit-up autoencoder models for the conclusive result of classification of exercises.

Acknowledgements This research was funded by the Department of Science and Technology DST under Biomedical Device and Technology Development (File No: TDP/BDTD/07/2021). We would like to render our sincere thanks to the Sri Ramachandra Institute of Higher Education and Research for their kind support and assistance in data acquisition. The study was conducted according to the guidelines of the Declaration of Helsinki and approved by the Institutional Ethics Committee of Sri Ramachandra Institute of Higher Education and Research with reference: IEC/22/APR/171/28 dated 17.05.2022.

Declarations

Conflict of interest The authors declare no conflict of interest.

References

Ahmad, N., Ghazilla, R.A.R., Khairi, N.M., Kasi, V.: Reviews on various inertial measurement unit (IMU) sensor applications. Int. J. Signal Process. Syst. (2013). https://doi.org/10.12720/ijsps.1.2.256-262

Al-Azzawi, S.S., Khaksar, S., Hadi, E.K., Agrawal, H., Murray, I.: HeadUp: a low-cost solution for tracking head movement of children with cerebral palsy using IMU. Sensors **21**(23), 8148 (2021). https://doi.org/10.3390/s21238148

Al-Ezzi, A., Al-Shargabi, A.A., Al-Shargie, F., Zahary, A.T.: Complexity analysis of EEG in patients with social anxiety disorder using fuzzy entropy and machine learning techniques. IEEE Access **10**, 39926–39938 (2022). https://doi.org/10.1109/ACCESS.2022.3165199

An, P., Wang, Z., Zhang, C.: Ensemble unsupervised autoencoders and Gaussian mixture model for cyberattack detection. Inf. Process. Manag. **59**(2), 102844 (2022). https://doi.org/10.1016/j.ipm.2021.102844

Antonio Santoyo-Ramón, J., Casilari, E., Manuel Cano-García, J.: A study of the influence of the sensor sampling frequency on the performance of wearable fall detectors. Measurement **193**, 110945 (2022). https://doi.org/10.1016/j.measurement.2022.110945

Boissonnault, J.S., Blaschak, M.J.: Incidence of diastasis recti abdominis during the childbearing year. Phys. Ther. **68**(7), 1082–1086 (1988). https://doi.org/10.1093/ptj/68.7.1082

Boukhennoufa, I., Zhai, X., Utti, V., Jackson, J., McDonald-Maier, K.D.: Wearable sensors and machine learning in post-stroke rehabilitation assessment: a systematic review. Biomed. Signal Process. Control **71**, 103197 (2022). https://doi.org/10.1016/j.bspc.2021.103197

Britnell, S.J., Cole, J.V., Isherwood, L., Stan, M.M., Britnell, N., Burgi, S., Candido, G., Watson, L.: Postural health in women: the role of physiotherapy. J. Obstet. Gynaecol. Can. **27**(5), 493–500 (2005). https://doi.org/10.1016/S1701-2163(16)30535-7

Chaurasia, S., Goyal, S., & Rajput, M.: Outlier detection using autoencoder ensembles: a robust unsupervised approach. In: 2020 International Conference on Contemporary Computing and Applications (IC3A), pp. 76–80 (2020). https://doi.org/10.1109/IC3A48958.2020.233273

Chiarello, C.M., Falzone, L.A., McCaslin, K.E., Patel, M.N., Ulery, K.R.: The effects of an exercise program on diastasis recti abdominis in pregnant women. J. Women's Health Phys. Therapy **29**(1), 11–16 (2005)

Chowdhury, A., Rosenthal, J., Waring, J., Umeton, R.: Applying self-supervised learning to medicine: review of the state of the art and medical implementations. Informatics **8**(3), 59 (2021). https://doi.org/10.3390/informatics8030059

Da Mota, P.G.F., Pascoal, A.G.B.A., Carita, A.I.A.D., Bø, K.: Prevalence and risk factors of diastasis recti abdominis from late pregnancy to 6 months postpartum, and relationship with lumbo-pelvic pain. Man. Ther. **20**(1), 200–205 (2015)

Du, Y.C., Shih, C.B., Fan, S.C., Lin, H.T., Chen, P.J.: An IMU-compensated skeletal tracking system using Kinect for the upper limb. Microsyst. Technol. **24**(10), 4317–4327 (2018). https://doi.org/10.1007/s00542-018-3769-6

Engh, M. E., Bø, K., Gluppe, S. B., Engh, M. E., & Bø, K.: Immediate effect of abdominal and pelvic floor muscle exercises on interrecti distance in women with diastasis recti abdominis who were parous. Phys. Therapy 100(8): 1372–1383 (2020). https://academic.oup.com/ptj/article/100/8/1372/5820961

Eriksson Crommert, M., Petrov Fieril, K., Gustavsson, C.: Women's experiences of living with increased inter-recti distance after childbirth: an interview study. BMC Womens Health **20**(1), 1–10 (2020). https://doi.org/10.1186/s12905-020-01123-1

Ganesan, Y., Gobee, S., Durairajah, V.: Development of an upper limb exoskeleton for rehabilitation with feedback from EMG and IMU sensor. Procedia Comput. Sci. **76**, 53–59 (2015). https://doi.org/10.1016/j.procs.2015.12.275

Han, Y., Ma, Y., Wang, J., Wang, J.: Research on ensemble model of anomaly detection based on autoencoder. In: 2020 IEEE 20th International Conference on Software Quality, Reliability and Security (QRS), pp. 414–417 (2020). https://doi.org/10.1109/QRS51102.2020.00060

Kadam, V.J., Jadhav, S.M.: Feature ensemble learning based on sparse autoencoders for diagnosis of Parkinson's disease. In: Computing, Communication and Signal Processing 2019, pp. 567–581. Springer, Singapore (2019)

Kong, W., Sessa, S., Cosentino, S., Zecca, M., Saito, K., Wang, C., Imtiaz, U., Lin, Z., Bartolomeo, L., Ishii, H., Ikai, T., Takanishi, A.: Development of a real-time IMU-based motion capture system for gait rehabilitation. IEEE Int. Conf. Robot. Biomim. (ROBIO) **2013**, 2100–2105 (2013). https://doi.org/10.1109/ROBIO.2013.6739779

Li, Z., Tian, L., Jiang, Q., Yan, X.: Distributed-ensemble stacked autoencoder model for non-linear process monitoring. Inf. Sci. **542**, 302–316 (2021). https://doi.org/10.1016/j.ins.2020.06.062

Liu, W., Jia, H., Wang, N., & Huang, Y.: Semi-supervised anomaly detection based on improved adversarial autoencoder and ensemble learning. In: 2021 4th International Conference on Advanced Electronic Materials, Computers and Software Engineering (AEMCSE), pp. 934–937 (2021). https://doi.org/10.1109/AEMCSE51986.2021.00190

Lopes, J., Simão, M., Mendes, N., Safeea, M., Afonso, J., Neto, P.: Hand/arm gesture segmentation by motion using IMU and EMG sensing. Procedia Manuf. **11**, 107–113 (2017). https://doi.org/10.1016/j.promfg.2017.07.158

Menaka, R., Karthik, R., Vinitha Joshy, P.: EMG-Based Analysis of Rehabilitation Exercises for Diastasis Recti Abdominis, Communication, Software and Networks, pp. 61–70. Springer, Singapore (2023)

Patel, S., Park, H., Bonato, P., Chan, L., Rodgers, M.: A review of wearable sensors and systems with application in rehabilitation. J. Neuro Eng. Rehabil. **9**(1), 21 (2012). https://doi.org/10.1186/1743-0003-9-21

Pintelas, P., Livieris, I.E.: Special issue on ensemble learning and applications. Algorithms **13**(6), 140 (2020). https://doi.org/10.3390/a13060140

Pulgar, F.J., Charte, F., Rivera, A.J., del Jesus, M.J.: ClEnDAE: A classifier based on ensembles with built-in dimensionality reduction through denoising autoencoders. Inf. Sci. **565**, 146–176 (2021). https://doi.org/10.1016/j.ins.2021.02.060

Qaroush, A., Yassin, S., Al-Nubani, A., Alqam, A.: Smart, comfortable wearable system for recognizing Arabic Sign Language in real-time using IMUs and features-based fusion. Expert Syst. Appl. **184**, 115448 (2021). https://doi.org/10.1016/j.eswa.2021.115448

Radhakrishnan, M., Ramamurthy, K.: Efficacy and challenges in the treatment of diastasis recti abdominis—a scoping review on the current trends and future perspectives. Diagnostics (2022). https://doi.org/10.3390/diagnostics12092044

Radhakrishnan, M., Ramamurthy, K., Kothandaraman, A., Premkumar, V.J., Ramesh, N.: Automatic assessment of abdominal exercises for the treatment of diastasis recti abdominis using electromyography and machine learning. Symmetry **14**(8), 1654 (2022). https://doi.org/10.3390/sym14081654

Saha, M., Santara, A., Mitra, P., Chakraborty, A., Nanjundiah, R.S.: Prediction of the Indian summer monsoon using a stacked autoencoder and ensemble regression model. Int. J. Forecast. **37**(1), 58–71 (2021). https://doi.org/10.1016/j.ijforecast.2020.03.001

Štebe, G., Krapež, P., Podobnik, J., Kogoj, D.: Trajectory tracking of an oscillating movement with a low-cost IMU in geodetic surveying applications. Measurement **176**, 109207 (2021). https://doi.org/10.1016/j.measurement.2021.109207

Thabet, A.A., Alshehri, M.A.: Efficacy of deep core stability exercise program in postpartum women with diastasis recti abdominis: a randomised controlled trial. J. Musculoskelet. Neuronal Interact. **19**(1), 62–68 (2019)